Information Contagion in Climate-Stressed SME Networks: An Agent-Based Simulation Study

Luong Doan
N2TP Technology Solutions JSC
Phenikaa University
Ha Noi, Viet Nam
21010345@st.phenikaa-uni.edu.vn

Uyen Nguyen
National Economics University
Ha Noi, Viet Nam
uyennt@neu.edu.vn

Thao Duong
East Asia University of Technology
Ha Noi, Viet Nam
thaodtp1@eaut.edu.vn

Ngan Duong
National Economics University
Ha Noi, Viet Nam
ch330429@st.neu.edu.vn

Phong Ho
N2TP Technology Solutions JSC
Ha Noi, Viet Nam
phong.ho@n2tp.com

Nhung Duong
Hanoi University of Pharmacy
N2TP Technology Solutions JSC
Ha Noi, Viet Nam
2312015@hup.edu.vn

Tuan Do
Phenikaa University
Ha Noi, Viet Nam
tuando7758@gmail.com

ABSTRACT

This paper investigates how heterogeneous adoption of environmental accounting standards generates information asymmetries that propagate through interconnected small and medium enterprise networks, creating emergent systemic vulnerabilities. We develop an agent-based model simulating hundreds of SMEs across multiple sectors, where firms adapt to climate stress based on differential access to environmental risk information. Our simulation framework captures the co-evolution of climate impacts, adaptation investments, and information diffusion through supply chain and credit network layers. Through extensive experiments, we identify a critical "valley of vulnerability" phenomenon where partial adoption of climate risk assessment tools temporarily increases systemic fragility before improving resilience. Spectral analysis reveals characteristic oscillation patterns in cascade dynamics that dampen with increased adoption. Robustness checks confirm this valley phenomenon emerges only when information signals are sufficiently precise to create behavioral divergence between informed and uninformed agents. Our findings challenge assumptions about gradual technology diffusion and provide quantitative insights for understanding information externalities in complex economic systems.

KEYWORDS

Agent-based modeling; Climate adaptation; Information asymmetry; Network contagion; SME resilience; Environmental accounting

Proc. of the 25th International Conference on Autonomous Agents and Multiagent Systems (AAMAS 2026), C. Amato, L. Dennis, V. Mascardi, J. Thangarajah (eds.), May 25 – 29, 2026, Paphos, Cyprus. © 2026 International Foundation for Autonomous Agents and Multiagent Systems (www.ifaamas.org). https://doi.org/10.65109/OCAP7538

ACM Reference Format:
Luong Doan, Uyen Nguyen, Thao Duong, Ngan Duong, Phong Ho, Nhung Duong, and Tuan Do. 2026. Information Contagion in Climate-Stressed SME Networks: An Agent-Based Simulation Study. In *Proc. of the 25th International Conference on Autonomous Agents and Multiagent Systems (AAMAS 2026), Paphos, Cyprus, May 25 – 29, 2026*, IFAAMAS, 9 pages. https://doi.org/10.65109/OCAP7538

1 INTRODUCTION

Climate change poses unprecedented challenges to economic systems, particularly for small and medium enterprises (SMEs) that comprise over 99% of European businesses and employ 65 million people. While large corporations increasingly adopt sophisticated environmental accounting systems, SMEs face significant barriers to climate risk assessment [15, 24], creating a heterogeneous information landscape that may amplify rather than mitigate systemic vulnerabilities. This paper examines how the partial adoption of Green Accounting and Business Analytics (GABA) standards generates information contagion effects through interconnected business networks, potentially creating systemic risks that exceed the sum of individual exposures.

The core insight driving our investigation is that information asymmetries in climate risk perception create behavioral externalities that propagate through supply chain and credit relationships [12, 28]. When only a subset of firms possesses accurate climate risk information, their adaptation decisions may inadvertently mislead less-informed neighbors, triggering cascading failures that would not occur under either complete ignorance or full information transparency. This phenomenon, which we term “information contagion,” operates through network channels where firms infer climate risks from their partners’ observable actions rather than accessing primary climate data [1].

We develop an agent-based model that captures the co-evolution of climate stress, adaptation investment, and information diffusion across a network of 200 SMEs calibrated to European sectoral data.

Each agent optimizes adaptation investments based on perceived climate risks, which depend on both their information capabilities (GABA adoption status) and signals received from network neighbors. The model incorporates realistic features including sectoral heterogeneity, multi-layer networks (supply chain and credit relationships), bounded rationality in risk perception, and spatially correlated climate shocks.

Our simulation experiments reveal two key findings. First, the relationship between GABA adoption and systemic resilience is non-monotonic, with partial adoption ($\lambda \in [0.25, 0.5]$) generating higher systemic capital losses than either minimal or complete adoption. Second, spectral analysis of resilience trajectories shows that information heterogeneity induces system-wide oscillations with characteristic frequencies around 5 months, which are progressively damped as adoption increases.

2 RELATED WORK

The intersection of climate risk, information asymmetry, and network contagion builds on three distinct literature streams. Financial contagion models, pioneered by Allen and Gale [3] and extended by Acemoglu et al. [2], demonstrate how network topology determines whether shocks remain localized or trigger systemic failures. Recent work by Xu [29] extends these frameworks by incorporating partial information in default cascades, while Peng and Zhang [22] examine how awareness-dependent behavioral adaptation affects contagion on multiplex networks. However, these models typically assume homogeneous information quality within informed subsets and focus on balance sheet contagion rather than behavioral adaptation. Our work extends this framework by incorporating heterogeneous information capabilities and endogenous adaptation decisions.

Climate economics literature, notably integrated assessment models by Nordhaus [21] and Stern [25], provides damage functions linking temperature increases to economic losses. Recent work by Hsiang et al. [13] emphasizes spatial heterogeneity in climate impacts, while Burke et al. [6] document non-linear temperature-productivity relationships. These macro-level analyses, however, abstract from firm-level adaptation decisions and information constraints that characterize SME responses to climate stress.

Agent-based modeling of climate adaptation has gained traction following Farmer et al.'s [11] call for complexity approaches to climate economics. Naumann-Woleske [20] provides a comprehensive review of agent-based integrated assessment models as alternatives to traditional equilibrium frameworks, highlighting their advantages in capturing heterogeneous agents and policy mixes. Lawyer et al. [17] review ABM applications to climate adaptation, emphasizing their utility in exploring emergent patterns at local scales. Lamperti et al. [16] model climate-economy feedbacks with heterogeneous agents, while Coronese et al. [10] specifically address SME vulnerabilities but assume perfect climate information. Our contribution lies in explicitly modeling information asymmetries and their network propagation effects.

The environmental accounting literature documents substantial heterogeneity in climate risk assessment capabilities. TCFD [27] reports that only 24% of European SMEs have adopted formal environmental accounting, creating what Christophers [9] terms "climate information inequality." Empirical studies by Hsu et al. [14] find that firms with better environmental disclosure show improved climate resilience, but network spillovers remain unexplored. Recent work emphasizes barriers to adoption including data inconsistency, lack of standardization, and resource constraints particularly acute for SMEs [15, 24].

Information asymmetry in supply chain networks has been shown to affect risk allocation and resilience in multiple contexts. Hou and Lu [12] demonstrate how information asymmetry and risk aversion interact to produce non-obvious risk allocation outcomes, while Wu and Pu [28] specifically address carbon information asymmetry and its implications for collaborative emission reduction. The social learning literature, particularly work on technology adoption through networks [1, 4], provides theoretical grounding for how firms infer risks from network neighbors' behaviors rather than direct observation. Our model operationalizes these information disparities and traces their systemic consequences through calibrated simulations.

Critically, our finding of non-monotonic adoption effects challenges classical innovation diffusion theory. Rogers [23] established the dominant framework assuming monotonic and beneficial progression of adoption. Recent work by Biancotti and Ciocca [5] suggests similar counter-intuitive patterns in cyber-financial systems, where mass adoption of simple technologies can increase systemic risk more than selective adoption of advanced technologies, hinting at non-monotonic effects that emerge from information heterogeneity in complex systems.

3 MODEL ARCHITECTURE

We model a directed multi-layer network $\mathcal{G} = (\mathcal{V}, \mathcal{E})$ where $\mathcal{V}$ represents $N = 200$ SME agents and $\mathcal{E}$ denotes weighted business relationships across supply chain and credit layers. Each agent i maintains state variables for capital $K_i(t)$, climate stress $T_i(t)$, and adaptation level $\alpha_i(t)$, with GABA adoption status $\theta_i \in \{0, 1\}$ determining information quality. The network structure captures empirically-grounded features of European SME ecosystems, including power-law degree distributions [8, 30] and sectoral clustering.

Although we calibrate to European SME ecosystems for concreteness, the framework is modular by design. Network topology (degree distribution, clustering coefficients, layer weights), sectoral parameters (composition, inter-sectoral trade flows), and interaction structures (damage functions, information channels) are all specified via configuration inputs rather than hard-coded. The core mechanism under study (information asymmetry propagation through heterogeneous networks) is not specific to SMEs or to climate stress, and the same architecture can be re-parameterized for other settings where partial technology adoption creates behavioral divergence among interconnected agents.

3.1 Agent Dynamics

Capital evolution follows:

$$\frac{dK_i}{dt} = s_i Y_i(t) - \delta K_i(t) - D_i(T_i, \alpha_i, K_i) - I_i(t) \tag{1}$$

where s_i is the firm-specific savings rate, δ is capital depreciation, D_i is climate damage (defined below), and $I_i(t)$ is the firm's adaptation investment (detailed in Section 3.3). Production $Y_i = A_i K_i^{0.33}$

uses Cobb-Douglas technology with diminishing returns to capital. Climate damage takes the quadratic-exponential form:

$$D_i(T_i, \alpha_i, K_i) = K_i \cdot [1 - \exp(-\omega T_i^2)] \cdot (1 - \beta\alpha_i)^\nu \quad (2)$$

The damage intensity coefficient $\omega = 0.033$ is calibrated to match IPCC projections of 3.3% annual damages by 2050 under moderate warming scenarios [13]. The adaptation effectiveness parameter $\beta = 0.5$ and elasticity $\nu = 1.2$ reflect empirical estimates of defensive investment efficacy [18, 19, 26]. This functional form captures accelerating climate damages at higher stress levels while allowing adaptation to partially mitigate these losses.

Climate stress accumulates through firm-level emissions, exogenous shocks, and natural decay, partially offset by adaptation investments:

$$\frac{dT_i}{dt} = \epsilon_Y Y_i(t) + \xi_i(t) - \mu_T T_i(t) - \kappa\alpha_i^\eta \quad (3)$$

where $\epsilon_Y = 0.02$ represents the emissions-output ratio, $\mu_T = 0.1$ captures natural stress dissipation, and the adaptation mitigation term uses $\kappa = 0.1$, $\eta = 1.5$ to model non-linear effectiveness of defensive measures. Stochastic shocks $\xi_i(t) \sim \mathcal{N}(0, \sigma^2_{\text{climate}})$ with $\sigma_{\text{climate}} = 0.05$ represent spatially and sectorally correlated climate events, generated via Cholesky decomposition of the correlation matrix:

$$\rho_{ij} = \exp\left(-\frac{d_{ij}^{\text{geo}}}{\ell_{\text{geo}}} - \frac{d_{ij}^{\text{sector}}}{\ell_{\text{sector}}}\right) \quad (4)$$

with length scales $\ell_{\text{geo}} = 100$ km and $\ell_{\text{sector}} = 1.5$ calibrated to regional climate data.

Adaptation capital evolves according to:

$$\frac{d\alpha_i}{dt} = \phi I_i(t)^\psi - \zeta\alpha_i(t) \quad (5)$$

where investment efficiency $\phi = 0.5$, elasticity $\psi = 0.8$, and depreciation rate $\zeta = 0.05$ determine the accumulation dynamics. This specification embeds diminishing returns to adaptation investment and gradual obsolescence of defensive measures.

The dynamics above are purely mechanical: under identical information, all firms would respond similarly to any level of climate stress. What differentiates outcomes across the network is how firms perceive that stress, a process governed by the information architecture described next.

3.2 Information Architecture

Agents perceive climate risk through noisy signals whose precision depends critically on GABA adoption. The perceived risk $\pi_i(t) \in [0, 1]$ updates according to:

$$\pi_i(t) = (1 - \gamma)\left[\theta_i \pi_i^{\text{local}}(t) + (1 - \theta_i)\pi_i^{\text{network}}(t)\right] + \gamma\pi_{\text{baseline}} \quad (6)$$

Equation 6 encodes the central information asymmetry. GABA adopters form beliefs from direct climate measurements (π_i^{local}), while non-adopters must infer risk indirectly from their business partners' observable financial performance (π_i^{network}), a much noisier channel. The decay term $\gamma\pi_{\text{baseline}}$ captures agents' tendency to revert toward a baseline prior ($\pi_{\text{baseline}} = 0.5$) in the absence of fresh signals, with $\gamma = 0.3$ governing the speed of this reversion.

where the decay rate $\gamma = 0.3$ governs regression toward a baseline prior $\pi_{\text{baseline}} = 0.5$.

For GABA adopters ($\theta_i = 1$), local signals combine direct climate observations with analytical tools:

$$\pi_i^{\text{local}} = \frac{T_i}{T_{\max}} + \epsilon_i^{\text{GABA}}, \quad \epsilon_i^{\text{GABA}} \sim \mathcal{N}(0, \tau_{\text{GABA}}^{-1}) \quad (7)$$

with precision $\tau_{\text{GABA}} = 4.0$ (equivalent to standard deviation 0.5). In practical terms, higher τ means the GABA signal tracks true climate stress more faithfully, allowing adopters to calibrate adaptation investments with greater confidence. Non-adopters ($\theta_i = 0$) rely on network inference [1], aggregating performance signals from business partners:

$$\pi_i^{\text{network}} = \sum_{j \in \mathcal{N}_i} \tilde{w}_{ij} \cdot \frac{1}{1 + \exp(-\rho\Delta K_j)} \quad (8)$$

where $\tilde{w}_{ij} = w_{ij} / \sum_{k \in \mathcal{N}_i} w_{ik}$ represents normalized influence weights combining supply chain ($w_{\text{supply}} = 0.6$) and credit relationships ($w_{\text{credit}} = 0.4$), $\Delta K_j = K_j(t) - K_j(t-1)$ captures recent capital changes, and $\rho = 5.0$ governs the sensitivity of belief formation to neighbor performance. This formulation embeds bounded rationality: agents cannot distinguish signal quality from partners and attribute capital losses to climate stress even when caused by other factors.

To illustrate: if firm j suffers a capital loss due to a supply chain disruption unrelated to climate, its non-adopting neighbor i nonetheless interprets this as evidence of elevated climate risk and adjusts its own adaptation investment accordingly. This attribution error is the micro-level mechanism through which information contagion originates. When many non-adopters simultaneously misread their neighbors' capital fluctuations, the resulting over- or under-investment propagates through the network as a cascade.

3.3 Adaptation Optimization

While the full optimization problem involves solving the Hamilton-Jacobi-Bellman equation for the value function $V_i(K_i, T_i, \alpha_i; \pi_i)$ [7], computational constraints for large-scale experiments necessitate a tractable approximation. We implement a calibrated heuristic that captures key behavioral patterns while reducing computational cost by approximately 50×:

$$I_i^* = \min\{L_i, L_i \cdot \eta_i(0.6s_i + 0.4g_i) + 0.1K_i g_i\} \quad (9)$$

where available liquidity $L_i = \psi_i K_i$ imposes a budget constraint with $\psi_i = 0.4$. The normalized stress signal $s_i = T_i/(1 + T_i^{\text{exp}})$ uses expected stress T_i^{exp} to temper extreme values, while the adaptation gap $g_i = \max\{0, \bar{\alpha}(s_i) - \alpha_i\}$ compares current adaptation against a target level $\bar{\alpha}(s_i) = \text{clip}(0.2 + 0.5s_i, 0, 1)$. Agent-specific adaptation propensity η_i introduces behavioral heterogeneity, with values drawn from $\mathcal{N}(1.0, 0.2^2)$ truncated to $[0.5, 1.5]$.

The heuristic allocates a liquidity share weighted 60% by current stress and 40% by the adaptation gap, plus a capital-proportional boost for under-adapted firms. This rule tends to produce more conservative adaptation investments than full optimization but preserves the qualitative stress-response relationship essential for studying information contagion effects. Robustness checks (Protocol 5, Section 4) confirm that alternative decision rules (stress-only triggers, payoff-threshold comparisons) modulate valley depth but

do not eliminate the core phenomenon, demonstrating that findings are robust to micro-level behavioral specifications. The heuristic can be toggled to the full HJB solver via configuration for validation purposes.

4 EXPERIMENTAL DESIGN

Our experimental framework employs a fractional factorial design optimized for local workstation computation, systematically varying GABA adoption rates $\lambda \in \{0, 0.125, 0.25, \ldots, 1.0\}$ (9 levels) and climate intensity $\omega \in \{0.025, 0.04\}$ (2 levels). Each configuration runs 20 Monte Carlo replications with distinct network realizations but consistent sectoral composition calibrated to Eurostat data, yielding 360 baseline simulations. Each simulation spans 120 months with time step $\Delta t = 0.25$ months, using 4th-order Runge-Kutta integration for state evolution.

4.1 Network Generation and Calibration

Network generation follows a multi-layer approach capturing empirical SME network structure. Agents are first assigned to sectors (manufacturing, services, construction, agriculture) following European SME distribution. Supply chain edges use a configuration model with power-law degree distribution $P(k) \sim (k+2)^{-2.3}$ within sectors [8], plus preferential attachment across sectors weighted by inter-sectoral trade flows. Credit relationships follow a spatial-sectoral proximity model:

$$P(e_{ij}^{\text{credit}} = 1) = \frac{1}{1 + \exp(a_0 + a_1 d_{ij} + a_2 \mathbb{1}[s_i \neq s_j])} \tag{10}$$

where d_{ij} represents geographic distance and $\mathbb{1}[s_i \neq s_j]$ penalizes cross-sector credit links.

Initial GABA adoption follows a logistic model incorporating capital and network position:

$$P(\theta_i = 1) = [1 + \exp(-\beta_0 - \beta_1 \log K_i - \beta_2 k_i)]^{-1} \tag{11}$$

with coefficients $\boldsymbol{\beta}$ calibrated via grid search to achieve target adoption rate λ while matching the empirical finding that larger, better-connected firms adopt preferentially. Initial capital stocks are drawn from log-normal distributions $\log K_i \sim \mathcal{N}(\mu_s, \sigma_s^2)$ with sector-specific parameters matching Eurostat SME size distributions.

4.2 Experimental Protocols

Protocol 1 (Main Effects): Two-way factorial design crossing adoption rates and climate intensity. Systemic capital loss serves as the primary response variable, with information entropy and adaptation efficiency gap as secondary outcomes. Two-way ANOVA isolates main effects and interactions.

Protocol 2 (Cascade Analysis): For adoption levels that $\lambda \in \{0.10, 0.24, 0.50, 0.75\}$, we inject uniform stress shocks of magnitude $2\sigma_{\text{climate}}$ at $t = 60$ months, sustaining for 12 months before linear recovery over 12 months. This protocol runs 20 replications per adoption level. We compute resilience metrics including normalized drop, recovery time, resilience area-under-curve, spectral characteristics via FFT of resilience trajectories, loss duration above baseline, and peak systemic capital loss.

Protocol 3 (Adoption Strategies): Eight targeting heuristics (random, degree, betweenness, eigenvector, sector, low-clustering, exposure-liquidity, climate-risk) pre-seed GABA adoption before simulation. Twenty replications per strategy enable one-way parametric ANOVA on max resilience drop and resilience AUC.

Table 1: Two-Way ANOVA for Systemic Capital Loss

Source	*Sum of Sq.*	*df*	*F-stat*	*p-value*
GABA adoption (λ)	1.497	5	18,320	$< 10^{-300}$
Climate intensity (ω)	0.000163	1	10.0	0.002
Residual	0.00381	233	—	—

4.3 Robustness and Validation Protocols

To ensure robustness of our core findings, we conduct extensive sensitivity analyses across multiple dimensions:

Protocol 4 (Scale Invariance): Test whether results hold across network sizes $N \in \{100, 200, 500\}$ crossed with adoption levels $\lambda \in \{0, 0.375, 0.5, 0.625, 0.75, 1.0\}$. Two-way ANOVA assesses whether agent count influences systemic outcomes or interacts with adoption effects. Five replications per cell yield 90 simulations.

Protocol 5 (Decision Heuristics): Evaluate three decision modes (baseline heuristic, stress-only trigger, payoff-threshold comparison) across the same adoption grid. Two-way ANOVA (heuristic $\times$ adoption level) tests whether behavioral assumptions affect valley depth. Five replications per cell yield 90 simulations.

Protocol 6 (Heuristic Parameters): Perturb baseline weights and propensities by ±20%. Stress weights $\in \{0.48, 0.60, 0.72\}$ and propensity multipliers $\in \{0.8, 1.0, 1.2\}$ create a 3×3 parameter grid crossed with adoption levels. This sweep assesses numerical stability of the valley phenomenon.

Protocol 7 (Information Quality): Vary GABA signal precision $\tau_{\text{GABA}} \in \{2.0, 4.0, 6.0\}$ crossed with adoption levels. This stress test identifies boundary conditions for valley emergence by modulating the strength of information asymmetry. We hypothesize that low-precision signals ($\tau = 2.0$) may eliminate the valley by reducing behavioral divergence between informed and uninformed agents.

All robustness protocols use aligned seeds across conditions to enable direct comparison. Together, these validation checks span 360 additional simulations beyond the 360 baseline runs, for a total experimental corpus of 720 simulations requiring approximately 72 hours on an 8-core workstation.

5 RESULTS

5.1 Non-Monotonic Adoption Effects

To isolate the relative importance of each experimental factor, we use analysis of variance (ANOVA), which decomposes total variation in the outcome into contributions from each factor; the resulting F-statistic measures the ratio of between-group to within-group variance, with larger values indicating stronger effects.

Analysis of variance reveals that GABA adoption rate dominates systemic outcomes ($F_{(5,233)} = 18{,}320$, $p < 10^{-300}$), while climate intensity provides secondary amplification ($F_{(1,233)} = 10.0$, $p = 0.002$). Table 1 presents the two-way ANOVA for systemic capital loss, our primary outcome measure.

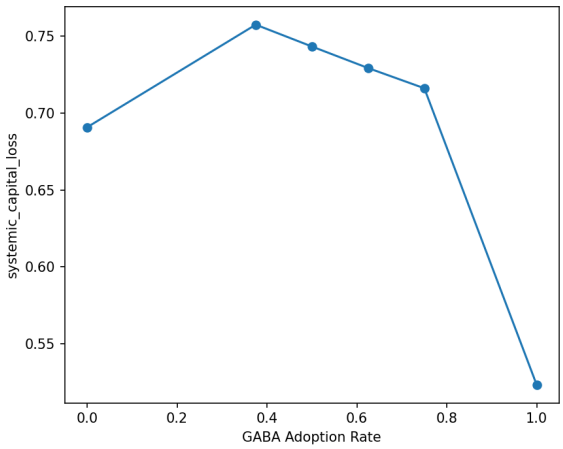

Figure 1: Valley of vulnerability in systemic capital loss. The inverted-U relationship between GABA adoption rate and systemic capital loss demonstrates that partial adoption temporarily increases systemic fragility before improving resilience.

Table 2: Mean Systemic Capital Loss by Adoption Rate and Climate Intensity

	Systemic Capital Loss		
λ	$\omega = 0.025$	$\omega = 0.10$	*Mean*
0.000	0.691	0.691	0.691
0.375	0.758	0.757	0.758
0.500	0.744	0.743	0.743
0.625	0.731	0.727	0.729
0.750	0.717	0.715	0.716
1.000	0.524	0.522	0.523

As shown in Figure 1 and Table 2, systemic capital loss exhibits a pronounced inverted-U relationship with adoption rate, peaking at $\lambda = 0.375$ with mean loss of 0.758 compared to 0.691 at zero adoption and 0.523 at full adoption.

This non-monotonic pattern emerges from competing mechanisms. At low adoption rates, most firms share similar (poor) information quality, leading to coordinated but suboptimal adaptation. As adoption increases to intermediate levels, information heterogeneity peaks. Though entropy decreases from 0.341 at $\lambda = 0$ to 0.165 at $\lambda = 0.375$ (Table 3), this intermediate state represents maximum behavioral divergence between GABA adopters and non-adopters rather than information disorder. The partial adopters create misleading signals: informed firms under-invest due to free-riding expectations while uninformed firms over-rely on distorted network signals. Only at high adoption rates does information convergence restore coordination, with entropy approaching zero at $\lambda = 1.0$.

The adaptation efficiency gap mirrors this pattern, peaking at 2.63 for $\lambda = 0.375$ before declining to 1.02 at full adoption, indicating that partial adoption generates the greatest misallocation

Table 3: Information Entropy and Adaptation Efficiency Gap

	Outcome Measures	
λ	*Info. Entropy*	*Adapt. Eff. Gap*
0.000	0.342	1.96
0.375	0.165	2.63
0.500	0.130	2.60
0.625	0.098	2.56
0.750	0.066	2.53
1.000	< 0.001	1.02

Table 4: Cascade Resilience Metrics by Adoption Level

	Spectral	*Recovery Metrics*				
λ	*FFT*	$\Delta\mathcal{R}_{norm}$	$T_R(90\%)$	*AUC*	T_{Loss}	*Bounce*
0.10	13.8	0.211	1.10	7.38	3.17	0.925
0.24	12.6	0.219	1.16	6.70	3.11	0.922
0.50	10.3	0.240	1.36	5.34	2.80	0.914
0.75	8.2	0.280	1.80	4.02	2.16	0.907

of defensive investments. Climate intensity amplifies these effects uniformly, adding approximately 0.002 to systemic losses across all adoption levels.

The preceding analysis characterizes steady-state outcomes. We now turn to dynamic behavior: how do these systems respond when hit by an acute climate shock, and what temporal signatures distinguish information-driven cascades from ordinary stress propagation?

5.2 Cascade Dynamics and Spectral Signatures

To characterize the temporal dynamics of information contagion, we apply Fourier analysis to resilience time series following an acute shock. This technique decomposes each trajectory into constituent oscillation frequencies, exposing periodic patterns in cascade behavior that are invisible in the aggregate statistics reported above. The analysis uncovers characteristic oscillations across all adoption levels, with a dominant frequency at 0.2 cycles/month (5-month period) whose amplitude decreases monotonically with adoption. Table 4 summarizes cascade metrics across adoption levels.

As illustrated in Figure 2, FFT magnitude at the dominant frequency drops from 13.8 at $\lambda = 0.10$ to 8.2 at $\lambda = 0.75$, demonstrating that information homogenization progressively dampens cascade propagation through the network. The 5-month period aligns with the timescale over which climate stress signals propagate through the supply chain layer, trigger adaptation responses in neighboring firms, and feed back into capital dynamics. This is broadly consistent with the quarterly-to-biannual adjustment cycles observed in SME business operations, suggesting the model captures a realistic propagation rhythm.

Recovery metrics show complex relationships with adoption. While resilience area-under-curve improves monotonically (decreasing from 7.38 to 4.02, where lower values indicate less cumulative loss), the normalized resilience drop $\Delta\mathcal{R}_{\text{norm}}$ counterintuitively

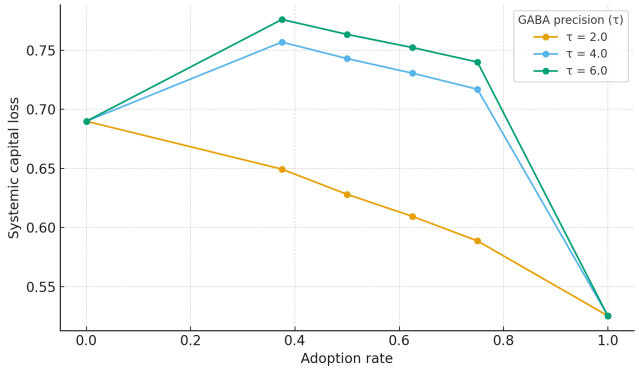

Figure 3: Boundary conditions for valley emergence. Systemic capital loss versus adoption rate under three levels of GABA signal precision demonstrates that information-driven vulnerability requires sufficiently strong signals to create behavioral divergence between informed and uninformed agents. All three conditions converge at full adoption, indicating that complete transparency eliminates precision dependency.

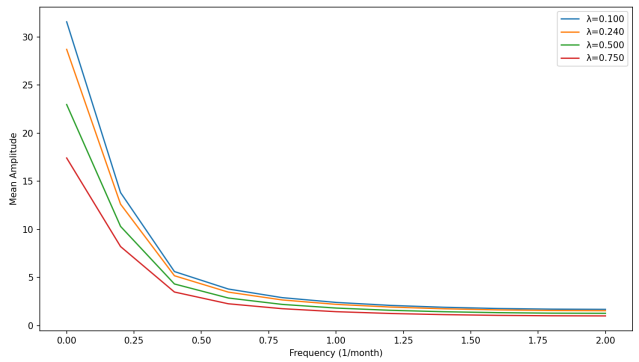

Figure 2: Fast Fourier Transform of resilience trajectories following uniform climate shock. Mean amplitude spectra across 20 replications show systematic damping of oscillations as GABA adoption increases, with dominant frequency at 0.2 cycles/month (5-month period). Higher adoption reduces amplitude by 41% (from 13.8 to 8.2), indicating stabilization of cascade dynamics.

increases with adoption (0.21 to 0.28). This apparent paradox resolves once we note that higher-adoption systems operate from stronger pre-shock baselines and therefore experience larger absolute disruptions when shocked, even though they recover faster. The normalized drop measures disruption relative to pre-shock performance, which naturally increases for systems starting from higher levels. Recovery time to 90% baseline similarly increases from 1.1 to 1.8 months, reflecting the longer path back to a higher equilibrium, though the bounce-back ratio remains stable around 0.91, indicating consistent recovery completeness regardless of adoption level.

Loss duration above baseline shows the clearest improvement, decreasing from 3.17 months at low adoption to 2.16 months at high adoption. This metric, combined with reduced oscillation amplitude, provides the strongest evidence that GABA adoption enhances systemic stability despite creating temporary vulnerabilities during transition periods.

Given that partial adoption amplifies systemic vulnerability, a natural policy question arises: does which firms adopt first matter? We investigate this by comparing targeted adoption strategies.

5.3 Strategic Adoption Patterns

Comparison of eight adoption targeting strategies reveals statistically significant differences in cascade mitigation ($F_{(7,152)} = 4.26$, $p = 0.0003$). Table 5 presents performance metrics across all strategies. Sector is significantly different from random baseline at $p < 0.05$ (one-way ANOVA with post-hoc Tukey HSD).

Sector-based targeting achieves the smallest maximum resilience drop (0.098) compared to random baseline (0.104), with climate-risk targeting close behind (0.101). Network centrality metrics (degree, betweenness, eigenvector) show intermediate performance, while exposure-liquidity targeting paradoxically performs worst (0.112).

The superior performance of sectoral targeting reflects the correlated shock structure of model where same-sector firms face similar climate stress. Concentrating GABA adoption within sectors creates local information consistency that prevents confusion from cross-sector signals. Climate-risk targeting succeeds by prioritizing firms already experiencing high stress who benefit most from accurate information.

The failure of exposure-liquidity targeting illustrates a subtle network effect: bolstering individually vulnerable firms without improving network-wide information quality merely shifts cascade initiation points without addressing propagation mechanisms. This finding challenges conventional "too-big-to-fail" intervention logic in the context of information-driven contagion.

5.4 Information Quality as Boundary Condition

Sensitivity analysis reveals that the valley of vulnerability is contingent on information signal quality, providing crucial insight into when this phenomenon emerges. Figure 3 demonstrates three distinct regimes based on GABA signal precision τ. With low-precision information ($\tau = 2.0$), systemic capital losses decrease monotonically from 0.690 to 0.525 as adoption increases, showing no valley formation. At baseline precision ($\tau = 4.0$), the characteristic valley emerges with losses peaking at 0.758 for $\lambda = 0.375$. Under high precision ($\tau = 6.0$), the valley deepens further, reaching 0.776 at partial adoption.

This finding establishes that information-driven systemic risk is not a universal property of heterogeneous adoption but requires signals potent enough to create sharp behavioral divergence. Weak signals ($\tau = 2.0$) provide insufficient differentiation to generate the miscoordination underlying cascade formation, while strong signals ($\tau = 6.0$) amplify the divergence between informed and uninformed agents, deepening the valley. The convergence at full adoption across all precision levels confirms that complete information transparency resolves the heterogeneity regardless of signal quality.

Table 5: Performance of GABA Adoption Targeting Strategies

	Performance Metrics		
Strategy	*Max Res. Drop*	*Res. AUC*	*Sys. Cap. Loss*
Random (baseline)	0.104	5.05	0.750
Sector	0.098*	5.16*	0.751
Climate-risk	0.101	5.11	0.750
Low-clustering	0.102	5.03	0.749
Eigenvector	0.102	5.08	0.750
Degree	0.105	5.07	0.750
Betweenness	0.104	5.02	0.749
Exposure-liquidity	0.112	5.02	0.750

6 DISCUSSION

6.1 Agent-Based Simulation Design

Our agent-based simulation approach reveals emergent phenomena that would remain invisible in equilibrium-based or representative-agent models. The valley of vulnerability emerges not from any individual agent's decision but from the collective interaction of heterogeneously informed agents navigating interconnected networks. This exemplifies the power of artificial societies methodology: by modeling individual decision-making under realistic constraints and allowing agents to interact through empirically-grounded networks, we uncover system-level patterns that contradict intuitive expectations about technology diffusion.

The simulation design deliberately incorporates multiple layers of heterogeneity to capture the complexity of real socio-economic systems. Agents differ in capital endowments (log-normal distributions by sector), network positions (power-law degree distributions), information capabilities (binary GABA adoption), and behavioral parameters (adaptation propensity drawn from truncated normal distributions). This multi-dimensional heterogeneity proves essential for the valley phenomenon: homogenizing any single dimension reduces but does not eliminate the effect, confirming that information asymmetry interacts with structural and behavioral diversity to generate systemic vulnerability.

The dominance of adoption rate over climate intensity (F-ratio of 1,832:1) demonstrates that social dynamics (specifically, information heterogeneity and its network propagation) matter more than physical environmental stress in determining systemic outcomes. This finding could only emerge from a simulation framework that explicitly models both the information architecture and the behavioral responses of individual agents.

The spectral analysis revealing characteristic 5-month oscillation periods provides a novel diagnostic tool that emerges from the temporal dynamics of agent interactions. These oscillations arise from the feedback loops between individual adaptation decisions and network-mediated information flows, creating a signature pattern that could potentially be detected in real economic data.

6.2 Calibration and Validation

Extensive sensitivity analyses confirm the robustness of the valley phenomenon while revealing important boundary conditions. Our validation strategy follows a three-tier approach: (1) parametric calibration to empirical targets, (2) structural validation through emergent pattern matching, and (3) systematic robustness testing across parameter spaces.

Climate damage intensity ($\omega = 0.033$) matches IPCC projections [13]. Network degree distributions ($P(k) \sim k^{-2.3}$) replicate observed SME supply chain structures [8]. Initial GABA adoption (24%) aligns with TCFD survey data [27]. Sectoral composition follows Eurostat SME distributions.

Scale invariance tests across network sizes (100–500 agents) demonstrate consistent patterns: two-way ANOVA shows adoption level dominates outcomes ($F_{(5,72)} = 1{,}921$, $p < 10^{-75}$) while agent count has negligible main effects ($F_{(2,72)} = 0.57$, $p = 0.57$). This insensitivity to population size suggests that the valley phenomenon is a structural property of the information-network interaction rather than an artifact of a particular scale, supporting applicability to ecosystems ranging from regional SME clusters of ∼100 firms to national-scale networks.

Most critically, information quality stress tests reveal that the valley is contingent on signal precision. With low-precision GABA signals ($\tau = 2.0$), systemic capital losses decrease monotonically. At baseline precision ($\tau = 4.0$), the characteristic valley emerges. Under high precision ($\tau = 6.0$), the valley deepens further. This demonstrates that information-driven systemic risk requires signals potent enough to create behavioral divergence.

6.3 Broader Applications

While our model focuses on climate adaptation in SME networks, the underlying mechanism (information heterogeneity creating systemic vulnerability through network effects) applies broadly to societal transitions involving distributed adoption of new capabilities. In public health, replacing firms with hospitals, capital with treatment capacity, and GABA with disease surveillance technology yields a system where partial adoption of early-warning tools could amplify epidemic cascades through referral and shared-resource networks. In financial markets, the architecture maps onto algorithmic trading adoption: firms with real-time analytics (adopters) and those relying on lagged market signals (non-adopters) interact through counterparty networks where the same information asymmetry generates correlated misallocation. In urban infrastructure, heterogeneous adoption of smart-grid or smart-traffic systems creates coordination failures analogous to the valley phenomenon when partially informed nodes issue signals that mislead their

uninformed neighbors. In each case, the model's modular inputs (network topology, information precision, damage functions) can be re-parameterized to the domain without altering the simulation engine.

The non-monotonic adoption effects we identify challenge classical innovation diffusion theory [23]. Recent work suggesting similar patterns in cyber-financial systems [5] supports our finding that information heterogeneity can temporarily increase systemic risk during technology transitions.

6.4 Methodological Contributions

The heuristic approximation of optimal control (reducing runtime while preserving key behavioral patterns) addresses a common challenge in large-scale agent-based simulations. Each agent would otherwise solve a high-dimensional Hamilton-Jacobi-Bellman equation [7] at every time step, creating an $O(N \times T \times D^3)$ computational burden where D is state space dimensionality. The calibrated heuristic reduces this to $O(N \times T)$ by encoding domain knowledge about stress-response and adaptation-gap dynamics directly into the decision rule. While the heuristic produces systematically lower adaptation investments than full optimization (reflecting conservative liquidity management), it preserves the qualitative response patterns essential for studying information heterogeneity effects. The model remains configurable to toggle between heuristic and HJB modes, allowing validation that core findings persist under both decision frameworks. This approach demonstrates how computational tractability can be achieved through behaviorally-motivated approximations that capture essential dynamics while enabling large-scale parameter exploration.

The integration of spectral analysis techniques with traditional aggregate metrics provides a richer characterization of system dynamics. Fast Fourier Transform analysis identifies dominant frequencies invisible in standard summary statistics. Our systematic exploration of boundary conditions demonstrates the importance of identifying when emergent phenomena will and will not manifest.

7 CONCLUSION

This paper demonstrates how heterogeneous adoption of environmental accounting standards generates information contagion that amplifies climate vulnerabilities in SME networks. Through comprehensive agent-based simulation, we establish three key contributions to understanding climate adaptation in complex economic systems.

First, we identify and characterize the "valley of vulnerability" phenomenon where partial adoption of climate risk assessment tools temporarily increases systemic fragility. This non-monotonic relationship between information capability and system resilience challenges linear diffusion models [23] and suggests that transition periods require careful management to avoid cascade amplification.

Second, we provide quantitative evidence that information architecture dominates physical climate intensity in determining systemic outcomes, with spectral analysis revealing characteristic oscillation signatures of information-driven cascades. These findings shift focus from climate forcing to information infrastructure as the primary determinant of economic resilience.

The robustness checks revealing that the valley emerges only under sufficient information precision add nuance to our findings: information-driven systemic risk is not universal but requires specific conditions where signals are strong enough to create behavioral divergence. This boundary condition strengthens our contribution by identifying precise circumstances under which intervention strategies must account for information heterogeneity effects.

Future research should explore several extensions. Incorporating learning dynamics could reveal whether systems naturally escape vulnerability valleys or require external coordination. Endogenous network rewiring [22] might identify self-organizing structures that enhance information transmission. Integration with empirical data on actual SME failures during climate events would validate model predictions and refine parameter calibration.

As climate stress intensifies and environmental disclosure requirements expand globally, understanding information contagion becomes critical for economic stability. Our results suggest that the path to climate resilience requires not just better information systems but coordinated deployment that accounts for network propagation effects. Policy makers must recognize that in interconnected economic systems, partial solutions may paradoxically increase vulnerability before reducing it.

REFERENCES

[1] Yazeed Abdul Mumin and Renan Goetz. 2025. Social learning and the acquisition of information and knowledge—a network approach for the case of technology adoption. *Oxford Economic Papers* 77, 1 (2025), 70–90.

[2] Daron Acemoglu, Asuman Ozdaglar, and Alireza Tahbaz-Salehi. 2015. Systemic risk and stability in financial networks. *American Economic Review* 105, 2 (2015), 564–608.

[3] Franklin Allen and Douglas Gale. 2000. Financial contagion. *Journal of Political Economy* 108, 1 (2000), 1–33.

[4] Pooria Assadi. 2024. Explaining Variation in Adoption of Organizational Innovation: A Social Network Approach. *Journal of International Technology and Information Management* (2024).

[5] Claudia Biancotti and Pierluigi Ciocca. 2018. Dry Rivers, Scary Strangers: Are Financial And Cyber Crises Alike? *Military Cyber Affairs* (2018).

[6] Marshall Burke, Solomon M Hsiang, and Edward Miguel. 2015. Global non-linear effect of temperature on economic production. *Nature* 527, 7577 (2015), 235–239.

[7] Alessandro Calvia, Fausto Gozzi, Francesco Lippi, and Giovanni Zanco. 2024. A simple planning problem for COVID-19 lockdown: a dynamic programming approach. *Economic Theory* 77, 1 (2024), 169–196.

[8] Abhijit Chakraborty and Yuichi Ikeda. 2020. Bow-tie structure and community identification of global supply chain network. *arXiv preprint arXiv:2006.14058* (2020).

[9] Brett Christophers. 2017. Climate change and financial instability: Risk disclosure and the problematics of neoliberal governance. *Annals of the American Association of Geographers* 107, 5 (2017), 1108–1127.

[10] Matteo Coronese, Francesco Lamperti, Klaus Keller, Francesca Chiaromonte, and Andrea Roventini. 2019. Evidence for sharp increase in the economic damages of extreme natural disasters. *Proceedings of the National Academy of Sciences* 116, 43 (2019), 21450–21455.

[11] J Doyne Farmer, Cameron Hepburn, Penny Mealy, and Alexander Teytelboym. 2015. A third wave in the economics of climate change. *Environmental and Resource Economics* 62, 2 (2015), 329–357.

[12] Chengfan Hou and Mengshi Lu. 2024. Allocating Inventory Risk in Retail Supply Chains: Risk Aversion, Information Asymmetry, and Outside Opportunity. *Manufacturing & Service Operations Management* 26 (2024), 1508–1525.

[13] Solomon Hsiang, Robert Kopp, Amir Jina, James Rising, Michael Delgado, Shashank Mohan, D J Rasmussen, Robert Muir-Wood, Paul Wilson, Michael Oppenheimer, et al. 2017. Estimating economic damage from climate change in the United States. *Science* 356, 6345 (2017), 1362–1369.

[14] Po-Hsuan Hsu, Kai Li, and Chi-Yang Tsou. 2023. The pollution premium. *The Journal of Finance* 78, 3 (2023), 1343–1392.

[15] Meny Huliselan. 2025. Environmental Accounting and Financial Management: A Strategic Approach to Corporate Sustainability. *Journal of Economics and Management Sciences* (2025), 164–170.

[16] Francesco Lamperti, Giovanni Dosi, Mauro Napoletano, Andrea Roventini, and Alessandro Sapio. 2018. Faraway, so close: Coupled climate and economic dynamics in an agent-based integrated assessment model. *Ecological Economics* 150 (2018), 315–339.

[17] Carly Lawyer, Li An, and Erfan Goharian. 2023. A Review of Climate Adaptation Impacts and Strategies in Coastal Communities: From Agent-Based Modeling towards a System of Systems Approach. *Water* (2023).
[18] Jacob Moscona and Karthik A Sastry. 2023. Does directed innovation mitigate climate damage? Evidence from US agriculture. *The Quarterly Journal of Economics* 138, 2 (2023), 637–701.
[19] A Narendr, BH Aithal, and Sutapa Das. 2024. A data-driven framework for enhancing coastal flood resilience in resource-crunched developing nations. *Geomatics, Natural Hazards and Risk* 15 (2024).
[20] Karl Naumann-Woleske. 2023. Agent-based Integrated Assessment Models: Alternative Foundations to the Environment-Energy-Economics Nexus.
[21] William D Nordhaus. 2017. Revisiting the social cost of carbon. *Proceedings of the National Academy of Sciences* 114, 7 (2017), 1518–1523.
[22] Xiao-Long Peng and Yi-Dan Zhang. 2021. Contagion dynamics on adaptive multiplex networks with awareness-dependent rewiring. *Chinese Physics B* 30, 5 (2021), 058901.
[23] Everett M Rogers. 1995. *Diffusion of innovations* (4th ed.). Free Press, New York.
[24] Khodor Shatila, Raissa Nurzhaubayeva, Natalia Malishevskaya, and Tatiana Podolskaya. 2024. Navigating sustainability: The role of environmental accounting in enhancing business performance. *E3S Web of Conferences* (2024).
[25] Nicholas Stern. 2007. *The economics of climate change: The Stern review.* Cambridge University Press.
[26] Timothy Sulser, Keith Wiebe, Shahnila Dunston, Nicola Cenacchi, Alejandro Nin-Pratt, Daniel Mason-D'Croz, Richard Robertson, Dirk Willenbockel, and Mark Rosegrant. 2021. Climate Change and hunger: Estimating costs of adaptation in the agrifood system.
[27] Task Force on Climate-related Financial Disclosures. 2022. *Task Force on Climate-related Financial Disclosures: 2022 Status Report.* Technical Report. Financial Stability Board.
[28] Xuezhong Wu and Xujin Pu. 2025. Blockchain technology adoption for collaborative emission reduction considering carbon information asymmetry in supply chains. *Kybernetes* 54, 6 (2025), 3460–3481.
[29] Yang Xu. 2019. Intervention on default contagion under partial information in a financial network. *PLoS ONE* 14 (2019).
[30] Weiwei Zhou and Qin Zhang. 2022. Resilience of supply-chain systems under perturbations: A network approach. *Chaos* 32, 9 (2022), 093123.